*Article*

# Spatial Distributions of Tropical Cyclone Tornadoes by Intensity and Size Characteristics

**Todd W. Moore** [1],* (iD), **Nicholas J. Sokol** [2] **and Robert A. Blume** [1]

1   Department of Geography and Environmental Planning, Towson University, 8000 York Road, Towson, MD 21252, USA; rblume1@students.towson.edu
2   Department of Geography, University of South Carolina, Callcott Building, 709 Bull Street, Columbia, SC 29208, USA; nsokol@email.sc.edu
*   Correspondence: tmoore@towson.edu; Tel.: +1-410-704-3973

**Abstract:** Tropical cyclones that make landfall often spawn tornadoes. Previous studies have shown that these tornadoes are not uniformly distributed in the United States or in the tropical cyclone environment. They show that tornadoes tend to occur relatively close to the coastline and that they tend to cluster to the east-of-center in the tropical cyclone environment, particularly in the northeast and east-of-center quadrants. This study contributes to these studies by analyzing the spatial distributions of tropical cyclone tornadoes by intensity, path length, path width, and the damage potential index. The analyses confirm that most tornadoes occur relatively close to the coastline, but show that stronger tornadoes with larger paths are disproportionately common farther inland. They also confirm that the highest amount of activity is located within the northeast and east-of-center quadrants and show that the most potentially damaging tornadoes cluster in a sub region near the intersection of these two quadrants.

**Keywords:** tropical cyclones; tornadoes; tropical cyclone tornado risk

## 1. Introduction

Tropical cyclones (TCs) produce tornadoes in the United States (US) along the Gulf and East Coastlines as they approach and make landfall, and at inland areas as they track into the midlatitudes. Similar to other TC hazards, these tornadoes threaten life and property. The tornadoes produced by TCs Earl (1998), Georges (1998), Mitch (1998), Bonnie (1998), Ivan (2004), and Rita (2005) were each responsible for 20+ casualties (fatalities + injuries) and, furthermore, TC tornadoes led to 328 casualties in the US over the period 1995–2009 [1]. The tornadoes produced by TC Cindy and other TCs in 2005 resulted in over an estimated $100 million (US) [2,3]. TC tornado risk is variable, not only because of variability in the number of tornadoes produced, but also because of a lack of awareness and often-complicated situations associated with TC preparation and evacuation. For example, TC tornadoes can be particularly hazardous at inland locations and at extended distances from TC center where other TC-related hazards are reduced and where preparedness and awareness are low [3,4]. It is, therefore, important to understand the components of TC tornado risk, including their spatial distributions.

Most TC tornadoes occur within 200–400 km of the coastline and within 12 h of landfall, but some are produced farther inland and days after landfall [3,5–7]. TC Ivan (2004), for example, produced an outbreak of tornadoes in the Mid-Atlantic Region of the US 1–2 days after landfall [8,9]. Within the TC environment, tornadoes are most common in the right half relative to TC motion, or in the east half relative to N (especially the NE quadrant) [3,6,7,10,11]. These sections (i.e., the right half and east half) often overlap [7], and are where shear and instability are most favorable for tornadogenesis.

Convective available potential energy (CAPE), which is an indicator of potential instability, tends to be greatest in the downshear section of TCs; in the northern hemisphere, the downshear section corresponds generally to the eastern half of TCs that are embedded in westerly shear [12,13]. Higher values of CAPE also have been reported in the right-front through left-rear (clockwise rotation) quadrants of tornadic TCs, as opposed to the left front quadrant [6], and elevated values of entraining CAPE have been reported in the northeast quadrant of tornadic TCs [14]. Helicity and shear parameters tend to be elevated in the downshear/eastern half of TCs [6,12,13].

While numerous studies have documented the spatial distribution of tornadoes within the TC environment, none have documented other tornado characteristics, such as damage rating (F/EF scale) and path length and width, within the TC environment. Documenting and analyzing the distributions of these characteristics is worthwhile because stronger tornadoes that cover larger areas pose greater societal risk. Furthermore, stronger tornadoes tend to occur in environments with higher values of instability and shear in non-TC and TC environments [7,15,16]. The enhanced instability and shear in the eastern portions of the TC environment may also increase the likelihood that the tornadoes that do occur are stronger and larger than those that are in the other portions. No studies have documented the distributions of these TC tornado characteristics in the broader US either. It is plausible that stronger and larger tornadoes occur more frequently as a TC tracks into more sheared higher latitude and inland locations.

In this study, we document and statistically analyze the spatial distributions of the F/EF scale rating, path length, path width, and destruction potential index (DPI) of tornadoes, both within the TC environment and in the US. The goals are to (1) document the spatial variability of these characteristics and (2) to determine if tornadoes tend to be stronger and larger at higher latitudes, farther inland, and in the eastern portions of the TC environment. We also provide a more thorough description of the distribution of DPI within the TC environment because of its potential to assess tornado risk [17,18].

## 2. Experiments

TC tornado data were collected from the tropical cyclone tornado (TCTOR) database [19], which is available at [20]; the README file is available at [21]. The TCTOR database is a compilation of data from the Storm Prediction Center's one-tornado (ONETOR) database and the National Hurricane Center's best-track records (HURDAT). The TC tornadoes within the database are verified to have been associated with a TC (tropical depression, tropical storm, hurricane, and remnant TCs) with surface- and upper-level maps, satellite photos, and/or NEXRAD Level II data. The database currently covers the 1995–2015 period, and includes 1296 tornadoes. Tornadoes with a recorded path width of 0 m were eliminated. There were 11 such tornadoes, which reduced the database to 1285 tornadoes. Multiple tornado and TC variables provided in TCTOR are considered in this study: latitude/longitude coordinates of the start and end of the tornadoes; bearing (degrees relative to N) of the tornadoes from TC center; range (km) of the tornadoes from TC center; tornado F/EF rating; path length (km) and width (m) of the tornadoes; and the DPI of the tornadoes. Details about the computation of the bearing and range of the TC tornadoes is provided in the README file and in the database itself. Path length is defined as the Euclidean distance between the start and end coordinates and the maximum observed path width has been recorded since 1994 [22]. The F- and EF-scales estimate wind speed based on observed damage. The F scale was used prior to 2007 and the EF scale has been used since. The two scales were designed to be consistent so that resulting inhomogeneities are minimized [23,24]. The DPI is a measure of the potential for casualties and property loss and, therefore, considers the path length, path width, and intensity of tornadoes. It is given by DPI = A(F + 1), where A is the area of the tornado path and F is the F- or EF-scale rating [25]).

The start latitude/longitude coordinates of the tornadoes were used to determine if the intensity and size characteristics of the tornadoes vary by latitude. To do so, the tornadoes were binned into the following categories: <30° N; 30° N–32° N; 32° N–34° N; >34° N. A non-parametric test was used to statistically evaluate the differences across the latitudinal categories because the distributions are

skewed. Most of the other distributions are also skewed, so non-parametric tests were used throughout the study. A Kruskal-Wallis test was used to determine if the mean ranks of tornado path length, path width, and DPI vary across the latitudinal categories. Post-hoc pairwise comparisons were performed with all Kruskal-Wallis tests. The significance threshold of the post-hoc tests were adjusted with the Bonferroni correction.

The start latitude/longitude coordinates of the tornadoes were also used to estimate their distance from the coastline. Once these distances were determined, the tornadoes were binned into the following categories: 0–100 km; 100–200 km; 200–300 km; >300 km. A Kruskal-Wallis test was used to determine if the mean ranks of tornado path length, path width, and DPI vary across the distance-from-coastline categories.

Four schemes were used to stratify the TC environment into regions to analyze the within-TC differences in tornado characteristics. The regions in the schemes are: (1) northeast (NE), southeast (SE), southwest (SW), and northwest (NW) quadrants (Figure 1a); (2) north of center (NoC), east of center (EoC), south of center (SoC), and west of center (WoC) (Figure 1b); (3) north half (NH) and south half (SH) (Figure 1c); east half (EH) and west half (WH) (Figure 1d). Each of the regions are defined relative to north. Tornadoes were binned into their respective regions using their bearing from the TC center. Kruskal-Wallis tests were used to determine if the mean ranks of tornado path length, path width, and DPI vary across the regions in the four-quadrant schemes (Figure 1a,b). Mann-Whitney tests were used to determine if these characteristics vary across the regions in the two-region schemes (Figure 1c,d).
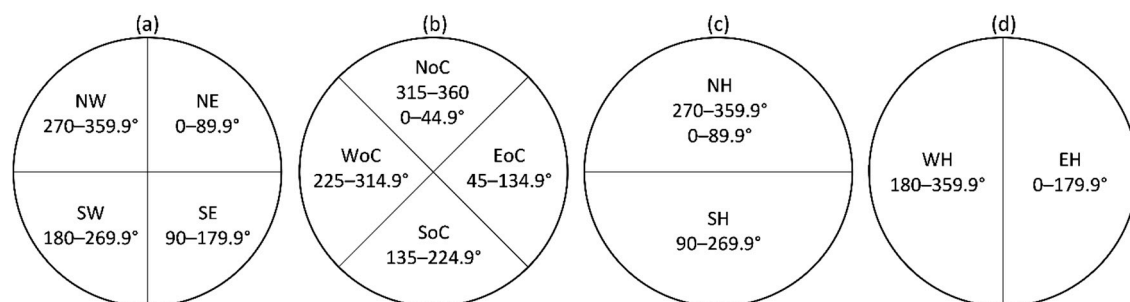


**Figure 1.** Illustration of the TC environment (circles) stratified into the different regions analyzed in this study. (**a**) shows the northeast (NE), southeast (SE), southwest (SW), and northwest (NW) sections; (**b**) shows the north of center (NoC), east of center (EoC), south of center (SoC), and west of center (WoC) sections; (**c**) shows the north half (NH) and south half (SH) sections; and (**d**) shows the west half (WH) and east half (EH) sections. The numerical ranges in degrees that define the sections are provided. All sections are defined relative to north.

## 3. Results

### 3.1. Spatial Distribution in the United States

#### 3.1.1. Latitude

The start locations of the 1285 tornadoes are shown in Figure 2. More intense and larger tornadoes appear to be more common at higher latitudes. The descriptive statistics in Table 1 support this observation. The proportion of tornadoes rated F/EF 2–3 increases with latitude, from 3% in the lowest latitude region to 9% in the highest. If considering the F/EF rating distribution of all 1285 TC tornadoes as the expected distribution, 94% should be weak F/EF 0–1 and 6% should be stronger F/EF 2–3. In comparison, there are fewer than expected strong tornadoes in the two lower latitude regions (i.e., <30° N and 30° N–32° N) and more than expected in the higher latitude regions (i.e., 32° N–34° N and >34° N).
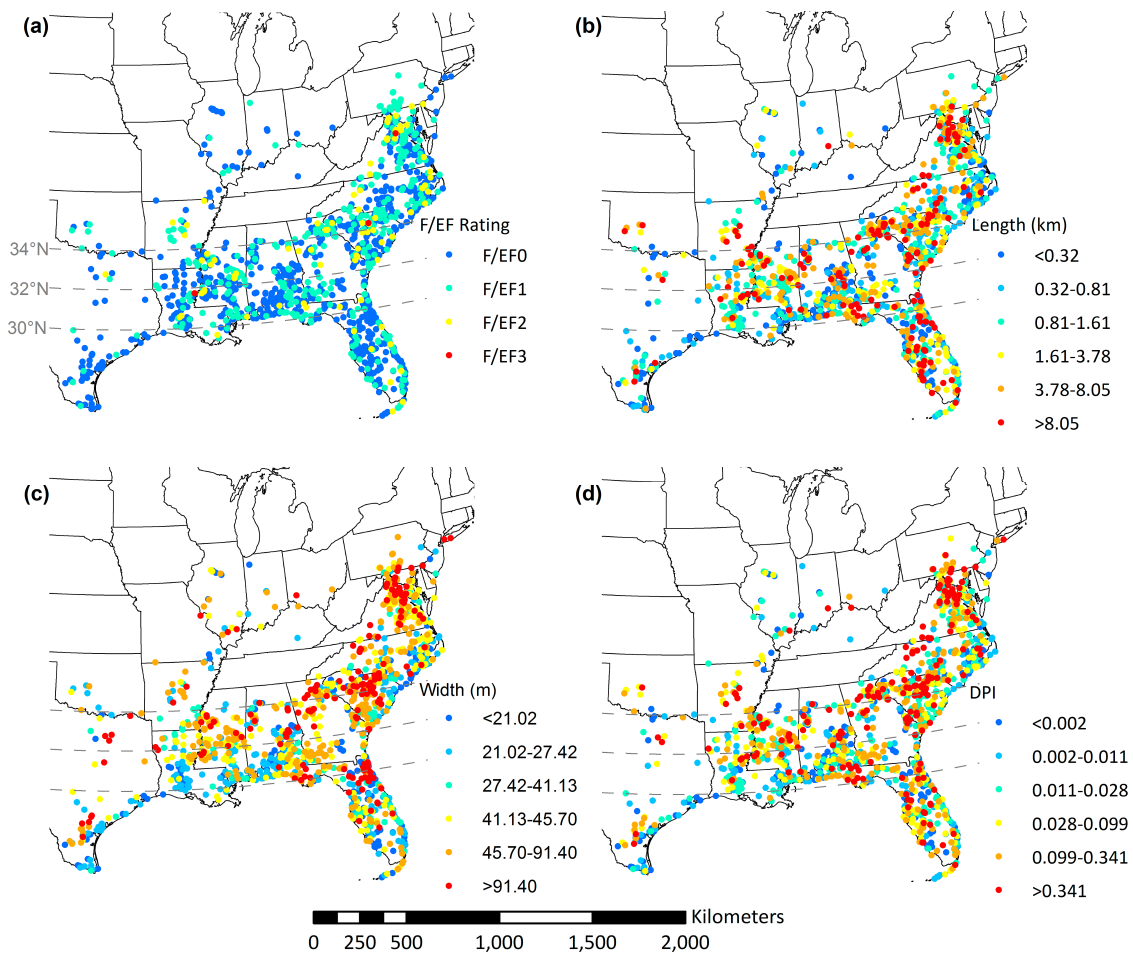
**Figure 2.** Spatial distribution of 1285 TC tornadoes, stratified by F/EF scale (**a**), path length (**b**), path width (**c**), and DPI (**d**). The distributions of length, width, and DPI are divided into quintiles.

The area covered by TC tornadoes also tends to increase with latitude. The median path length in the >34° N region is double the median in the <30° N, and median path width is nearly double. The median DPI in the two farthest north regions are six and five times greater than the median DPI in the farthest south regions. The Kruskal-Wallis test indicates that the differences in the mean ranks of these variables are statistically significant (Table 2). The post-hoc tests illustrate that the mean ranks of path length, path width, and DPI are significantly greater in the 32° N–34° N and >34° N regions than they are in the <30° N and 30° N–32° N regions.

**Table 1.** Descriptive statistics for the <30° N, 30° N–32° N, 32° N–34° N, and >34° N regions.

| Tornado Characteristic | <30° N (*n* = 273) | 30° N–32° N (*n* = 307) | 32° N–34° N (*n* = 266) | >34° N (*n* = 439) |
|---|---|---|---|---|
| **F/EF scale** | | | | |
| Weak (F/EF 0–1) | 264 (97%) | 295 (96%) | 244 (92%) | 399 (91%) |
| Strong (F/EF 2–3) | 9 (3%) | 12 (4%) | 22 (8%) | 40 (9%) |
| **Path length (km)** | | | | |
| Mean | 4.1 | 2.7 | 3.7 | 3.7 |
| Median | 0.8 | 1.2 | 1.6 | 1.6 |
| **Path width (m)** | | | | |
| Mean | 57.6 | 61.9 | 92.4 | 82.8 |
| Median | 27.4 | 27.4 | 45.7 | 45.7 |
| **DPI** | | | | |
| Mean | 0.15 | 0.27 | 0.52 | 0.42 |
| Median | 0.01 | 0.01 | 0.06 | 0.05 |

**Table 2.** Mean ranks used in the Kruskal-Wallis tests for the <30° N, 30° N–32° N, 32° N–34° N, and >34° N regions. Results of the Kruskal-Wallis tests are located below the table. Post-hoc pairwise comparisons indicate that, for all three variables, the mean ranks in the 32° N–34° N and >34° N regions are significantly greater than the mean ranks in the <30° N and 30° N–32° N regions.

| Tornado Characteristic | <30° N | 30° N–32° N | 32° N–34° N | >34° N |
|:---:|:---:|:---:|:---:|:---:|
| Path length (km) [a] | 570.1 | 583.9 | 712.4 | 687.6 |
| Path width (m) [b] | 495.3 | 550.1 | 769.5 | 723.2 |
| DPI [c] | 531.2 | 557.1 | 734.7 | 717.1 |

[a] $X^2 = 34.2$, $df = 3$, $p < 0.001$; [b] $X^2 = 115.4$, $df = 3$, $p < 0.001$; [c] $X^2 = 75.0$, $df = 3$, $p < 0.001$.

### 3.1.2. Distance from Coastline

It is apparent that most TC tornadoes occur in states adjacent to the Gulf or East Coastlines, and that strong and weak tornadoes have occurred at varying distances from the coastline. However, stronger tornadoes, with larger paths and greater DPIs, appear to occur farther inland more often. There are prominent groups of relatively strong and large tornadoes at inland areas (see Figure 2c,d). The grouping of tornadoes in southeast Arkansas, north Louisiana, and middle Mississippi have relatively wide tracks and large DPI values (see Appendix A for a map with state names). Other similar groupings include one in northeast Alabama and north Georgia and another running through the western portions of South Carolina, North Carolina, Virginia, and Maryland, to the east of the Appalachian Mountains.

The descriptive statistics in Table 3 illustrate that TC tornadoes tend to be more intense and larger at inland locations. The proportion of tornadoes rated F/EF 2–3 within 200 km of the coastline, at 5%, is close to the proportion of all TC tornadoes (6%). The proportion in the regions that are farther inland, however, are notably greater, at 10% each. The median path length, path width, and DPI markedly increase between the 0–100 km and 200–300 km regions, but then decrease into the farthest inland region (i.e., >300 km). The Kruskal-Wallis test indicates that the differences in the mean ranks of the variables are statistically significant (Table 4) and, furthermore, the post-hoc tests show that the mean ranks of all of the inland regions are greater than the mean ranks of the region closest to the coast.

**Table 3.** Descriptive statistics for the 0–100 km, 100–200 km, 200–300 km, and >300 km regions.

| Tornado Characteristic | 0–100 km (*n* = 634) | 100–200 km (*n* = 262) | 200–300 km (*n* = 203) | >300 km (*n* = 186) |
|:---:|:---:|:---:|:---:|:---:|
| **F/EF scale** | | | | |
| Weak (F/EF 0–1) | 604 (95%) | 248 (95%) | 182 (90%) | 168 (90%) |
| Strong (F/EF 2–3) | 30 (5%) | 14 (5%) | 21 (10%) | 18 (10%) |
| **Path length (km)** | | | | |
| Mean | 3.2 | 3.3 | 4.4 | 4.2 |
| Median | 0.8 | 1.6 | 2.4 | 1.6 |
| **Path width (m)** | | | | |
| Mean | 57.7 | 85.1 | 96.7 | 92.2 |
| Median | 27.4 | 45.7 | 68.6 | 45.7 |
| **DPI** | | | | |
| Mean | 0.20 | 0.36 | 0.51 | 0.64 |
| Median | 0.01 | 0.04 | 0.09 | 0.06 |

**Table 4.** Mean ranks used in the Kruskal-Wallis tests for the 0–100 km, 100–200 km, 200–300 km, and >300 km regions. Results of the Kruskal-Wallis tests are located below the table. Post-hoc pairwise comparisons indicate that, for all three variables, the mean ranks of the 100–200 km, 200–300 km, and >300 km regions are significantly greater than the mean ranks of the 0–100 km region.

| Tornado Characteristic | 0–100 km | 100–200 km | 200–300 km | >300 km |
|---|---|---|---|---|
| Path length (km) [a] | 563.8 | 693.4 | 764.7 | 709.1 |
| Path width (m) [b] | 519.6 | 735.5 | 800.1 | 761.9 |
| DPI [c] | 537.9 | 709.1 | 798.0 | 738.9 |

[a] $X^2 = 61.8$, $df = 3$, $p < 0.001$; [b] $X^2 = 143.7$, $df = 3$, $p < 0.001$; [c] $X^2 = 107.0$, $df = 3$, $p < 0.001$.

## 3.2. Spatial Distribution in the Tropical Cyclone Environment

Figure 3a–d shows the spatial distribution of the tornadoes and their characteristics within the TC environment. The concentration of tornadoes in the eastern portion, particularly the NE and/or EoC quadrants, of the TC environment is apparent. There is also visual evidence that tornadoes with longer and wider paths, greater F/EF ratings, and larger DPIs are not uniformly distributed across the TC environment. The distributions of these tornado characteristics across the TC regions that are presented in Figure 1 are described and analyzed in Sections 3.2.1–3.2.4.
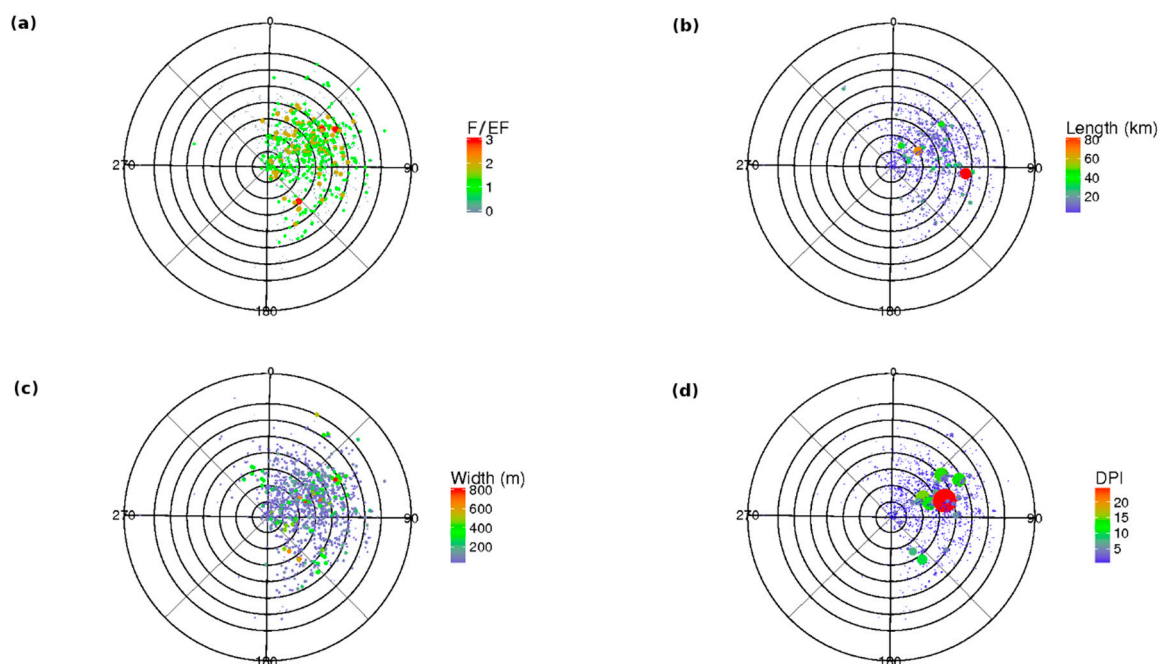


**Figure 3.** Spatial distribution of 1280 * tornadoes within the TC environment, stratified by F/EF scale (**a**), path length (**b**), path width (**c**), and DPI (**d**). Bearing in degrees is defined relative to north. Concentric range rings in km are place at an interval of 100 km. * Five tornadoes are not displayed because their ranges exceed 800 km.

### 3.2.1. Northeast (NE), Southeast (SE), Southwest (SW), and Northwest (NW) Quadrants

Of the 1285 tornadoes in the database, 67% ($n = 855$) were located in the NE quadrant of their respective TC, 27% ($n = 348$) in the SE quadrant, <1% ($n = 10$) in the SW quadrant, and 6% ($n = 72$) in the NW quadrant (Table 5). The tornadoes tended to be weak F/EF 0–1 in all quadrants, but stronger F/EF 2–3 tornadoes were relatively more common in the NE and SE quadrants, where they comprised 6–7% of all respective tornadoes. Only 1% of the tornadoes in the NW quadrant were rated strong, and none in the SW quadrant was rated strong.

Table 5 presents parametric and non-parametric statistics describing the central tendencies of tornado path length, path width, and DPI for the quadrants. The central tendencies of the NE and SE quadrants exceed those of the SW and NW quadrants, with the exception of the median path length in the SW quadrant. Kruskal-Wallis tests indicate that statistically significant differences exist between the mean ranks of path length, path width, and DPI in the four quadrants (Table 6). Post-hoc pairwise comparisons show more specifically that the differences exist between the NE and NW quadrants and between the SE and NW quadrants. The mean ranks of all variables are significantly greater in the NE and SE quadrants than in the NW quadrant. The mean ranks of the SW quadrant also are relatively large, especially for path length and DPI, but these are based on sample sizes of 10 and are inflated by outliers.

**Table 5.** Descriptive statistics for the northeast (NE), southeast (SE), southwest (SW), and northwest (NW) quadrants.

| Tornado Characteristic | NE Quadrant ($n$ = 855) | SE Quadrant ($n$ = 348) | SW Quadrant ($n$ = 10) | NW Quadrant ($n$ = 72) |
|---|---|---|---|---|
| **F/EF scale** | | | | |
| Weak (F/EF 0–1) | 794 (93%) | 327 (94%) | 10 (100%) | 71 (99%) |
| Strong (F/EF 2–3) | 61 (7%) | 21 (6%) | 0 (0%) | 1 (1%) |
| **Path length (km)** | | | | |
| Mean | 3.6 | 3.8 | 2.4 | 2.1 |
| Median | 1.6 | 1.6 | 2.3 | 0.8 |
| **Path width (m)** | | | | |
| Mean | 73.5 | 77.4 | 56.7 | 73.8 |
| Median | 45.7 | 45.7 | 25.1 | 27.4 |
| **DPI** | | | | |
| Mean | 0.40 | 0.26 | 0.11 | 0.12 |
| Median | 0.03 | 0.04 | 0.04 | 0.01 |

**Table 6.** Mean ranks used in the Kruskal-Wallis tests for the northeast (NE), southeast (SE), southwest (SW), and northwest (NW) quadrants. Results of the Kruskal-Wallis tests are located below the table. Post-hoc pairwise comparisons indicate that, for all three variables, the mean ranks of the NE and SE quadrants are significantly greater than the mean ranks of the NW quadrant.

| Tornado Characterisitc | NE Quadrant | SE Quadrant | SW Quadrant | NW Quadrant |
|---|---|---|---|---|
| Path length (km) [a] | 642.8 | 668.9 | 699.2 | 513.0 |
| Path width (m) [b] | 653.5 | 649.0 | 546.0 | 503.3 |
| DPI [c] | 646.4 | 665.1 | 634.4 | 497.6 |

[a] $X^2$ = 10.8, $df$ = 3, $p$ = 0.013; [b] $X^2$ = 11.8, $df$ = 3, $p$ = 0.008; [c] $X^2$ = 12.4, $df$ = 3, $p$ = 0.006.

### 3.2.2. North of Center (NoC), East of Center (EoC), South of Center (SoC), and West of Center (WoC) Quadrants

Twenty-six percent ($n$ = 333) of the tornadoes were located in the NoC quadrant, 65% ($n$ = 838) in the EoC quadrant, 8% ($n$ = 100) in the SoC quadrant, and 1% ($n$ = 14) in the WoC quadrant (Table 7). Weak F/EF 0–1 tornadoes accounted for >90% of all tornadoes in each quadrant. Stronger F/EF 2–3 tornadoes were relatively more common in the SoC quadrant, where they accounted for 10% of the tornadoes in the quadrant. Stronger tornadoes accounted for 6% of all tornadoes in the NoC and EoC quadrants; there were no strong tornadoes in the WoC quadrant.

Statistics describing the central tendency of path length, path width, and DPI in the four quadrants are presented in Table 7. The central tendencies are greatest in the EoC and SoC quadrants with the exception of the median path length, which is greatest in the WoC quadrant. The few tornadoes that occurred in the WoC quadrant were long-tracked, but had relatively narrow widths and were weak in intensity. Kruskal-Wallis tests indicate that there are significant differences between the mean ranks of the three variables across the quadrants (Table 8). Post-hoc comparisons specify that the mean ranks are significantly greater in the EoC and SoC quadrants than in the NoC quadrant.

**Table 7.** Descriptive statistics for the north-of-center (NoC), east-of-center (EoC), south-of-center (SoC), and west-of-center (WoC) quadrants.

| Tornado Characteristic | NoC Quadrant (*n* = 333) | EoC Quadrant (*n* = 838) | SoC Quadrant (*n* = 100) | WoC Quadrant (*n* = 14) |
|---|---|---|---|---|
| **F/EF scale** | | | | |
| Weak (F/EF 0–1) | 313 (94%) | 785 (94%) | 90 (90%) | 14 (100%) |
| Strong (F/EF 2–3) | 20 (6%) | 53 (6%) | 10 (10%) | 0 (0%) |
| **Path length (km)** | | | | |
| Mean | 2.8 | 3.8 | 3.7 | 2.8 |
| Median | 1.0 | 1.6 | 1.6 | 2.0 |
| **Path width (m)** | | | | |
| Mean | 56.2 | 80.0 | 89.5 | 69.1 |
| Median | 30.2 | 45.7 | 45.7 | 25.1 |
| **DPI** | | | | |
| Mean | 0.15 | 0.41 | 0.48 | 0.21 |
| Median | 0.01 | 0.03 | 0.04 | 0.02 |

**Table 8.** Mean ranks used in the Kruskal-Wallis tests for the north-of-center (NoC), east-of-center (EoC), south-of-center (SoC), and west-of-center (WoC) quadrants. Results of the Kruskal-Wallis tests are located below the table. Post-hoc pairwise comparisons indicate that, for all three variables, the mean ranks of the EoC and SoC quadrants are significantly greater than the mean rank of the NoC quadrant.

| Tornado Characteristic | NoC Quadrant | EoC Quadrant | SoC Quadrant | WoC Quadrant |
|---|---|---|---|---|
| Path length (km) [a] | 580.8 | 662.0 | 688.0 | 661.8 |
| Path width (m) [b] | 544.4 | 679.4 | 690.6 | 468.9 |
| DPI [c] | 562.0 | 670.5 | 690.7 | 581.8 |

[a] $X^2 = 13.2$, $df = 3$, $p = 0.004$; [b] $X^2 = 36.8$, $df = 3$, $p < 0.001$; [c] $X^2 = 22.5$, $df = 3$, $p < 0.001$.

### 3.2.3. North Half (NH) and South Half (SH)

Seventy-two percent (*n* = 927) of the tornadoes occurred in the NH of the TC environment and 28% (*n* = 358) occurred in the SH (Table 9). There is no difference in the proportion of tornadoes by F/EF scale between the halves. Weaker F/EF 0–1 tornadoes accounted for 93–94% of tornadoes in both halves and stronger F/EF 2–3 tornadoes accounted for 6–7%. Differences in the central tendency metrics also are not as evident as they are with the quadrant stratifications. Moreover, Mann-Whitney *U* tests indicate that there are no statistically significant differences between the halves, with any variable (Table 10).

**Table 9.** Descriptive statistics for the north and south halves (NH and SH, respectively).

| Tornado Characterisitc | NH (*n* = 927) | SH (*n* = 358) |
|---|---|---|
| **F/EF scale** | | |
| Weak (F/EF 0–1) | 865 (93%) | 337 (94%) |
| Strong (F/EF 2–3) | 62 (7%) | 21 (6%) |
| **Path length (km)** | | |
| Mean | 3.5 | 3.7 |
| Median | 1.6 | 1.6 |
| **Path width (m)** | | |
| Mean | 73.5 | 76.8 |
| Median | 45.7 | 45.7 |
| **DPI** | | |
| Mean | 0.38 | 0.26 |
| Median | 0.03 | 0.04 |

**Table 10.** Mean ranks used in the Mann-Whitney tests for the north half (NH) and south half (SH). Results of the Mann-Whitney tests are located below the table.

| Tornado Characteristic | NH | SH |
|---|---|---|
| Path length (km) [a] | 632.7 | 669.7 |
| Path width (m) [b] | 641.8 | 646.2 |
| DPI [c] | 634.8 | 664.2 |

[a] $U = 175{,}505$, $p = 0.107$; [b] $U = 231{,}321$, $p = 0.849$; [c] $U = 173{,}529$, $p = 0.203$.

### 3.2.4. East Half (EH) and West Half (WH)

Ninety-four percent ($n = 1203$) of the tornadoes occurred in the EH of the tropical cyclone environment and 6% ($n = 82$) occurred in the WH (Table 11). As expected after the NE, SE, SW, and NW stratification, the proportion of strong tornadoes (i.e., F/EF 1–2) is notably greater in the EH. The central tendency metrics also are greater in the EH. Mann-Whitney $U$ tests indicate that the mean ranks of all variables are significantly greater in the EH (Table 12).

**Table 11.** Descriptive statistics for the east and west halves (EH and WH, respectively).

| Tornado Characteristic | EH ($n = 1203$) | WH ($n = 82$) |
|---|---|---|
| **F/EF scale** | | |
| Weak (F/EF 0–1) | 1121 (93%) | 81 (>99%) |
| Strong (F/EF 2–3) | 82 (7%) | 1 (<1%) |
| **Path length (km)** | | |
| Mean | 3.6 | 2.1 |
| Median | 1.6 | 0.8 |
| **Path width (m)** | | |
| Mean | 74.6 | 71.7 |
| Median | 45.7 | 27.4 |
| **DPI** | | |
| Mean | 0.36 | 0.11 |
| Median | 0.03 | 0.01 |

**Table 12.** Mean ranks used in the Mann-Whitney tests for the east half (EH) and west half (WH). Results of the Mann-Whitney tests are located below the table.

| Tornado Characteristic | EH | WH |
|---|---|---|
| Path length (km) [a] | 650.3 | 535.7 |
| Path width (m) [b] | 652.2 | 508.6 |
| DPI [c] | 651.8 | 514.3 |

[a] $U = 40{,}523$, $p = 0.007$; [b] $U = 38{,}299$, $p = 0.001$; [c] $U = 38{,}770$, $p = 0.001$.

### 3.2.5. Destruction Potential Index (DPI)

DPI is a measure of the potential for tornado-related casualties and losses, and is a function of the area covered by a tornado's path and its intensity (as estimated with the F/EF scale) [25]. It puts an emphasis on strong and violent, long- and wide-tracked tornadoes that are most likely to cause the greatest damage and, therefore, pose the greatest societal risk [17,18]. Due to its utility in assessing tornado risk, the DPI of the TC tornadoes is described in more detail here.

DPI ranges from $2.84 \times 10^{-5}$ to 24.55 and is positively skewed (Figure 4). The DPI of 117 tornadoes exceeds the 90th percentile of 0.68. All except three of these extreme DPI tornadoes occurred in the EH of the tornado environment, mostly in the NE and/or EoC quadrants (Figure 3d). The central 50% of the tornadoes, or those bound between the 25th and 75th percentiles of bearing and range, occurred between 53° and 86° from N and between 285 km and 423 km from TC center; the median center

(bearing, range) is 65°, 353 km. Moreover, eight of the ten tornadoes (and ties) with the highest DPIs occurred in this same general region (Table 13; also see the cluster of green and red circles in the NE quadrant of Figure 3d). These tornadoes were produced by multiple TCs, suggesting a propensity for the most potentially damaging tornadoes to occur in this region of the TC environment.

　　Table 13 illustrates that the most potentially damaging tornadoes can have various size and intensity combinations. The tornado with the largest DPI had a path length of 29 km and width of 731 m, and was rated as F 2 with estimated wind speeds between 182 and 253 km h$^{-1}$. Most of the other tornadoes also had path widths in excess of 400 m. The one tornado with the narrowest width had the longest path (length = 68 km). Table 13 also shows that the most potentially damaging tornadoes resulted in only 18 casualties. The five TC tornadoes with the most casualties (10 or more) had DPI values of 4.26 or less; three of them had values of less than 1. The greatest casualty count is 32, which is related to one of TC Bonnie's (2004) F 2 tornadoes with a path length of 8 km, path width of 457 m, and DPI of 4.26. This tornado intersected multiple residential areas, which illustrates that tornado-related losses are a function of the size and intensity of a tornado along with the impacted socioeconomic landscape [26,27].
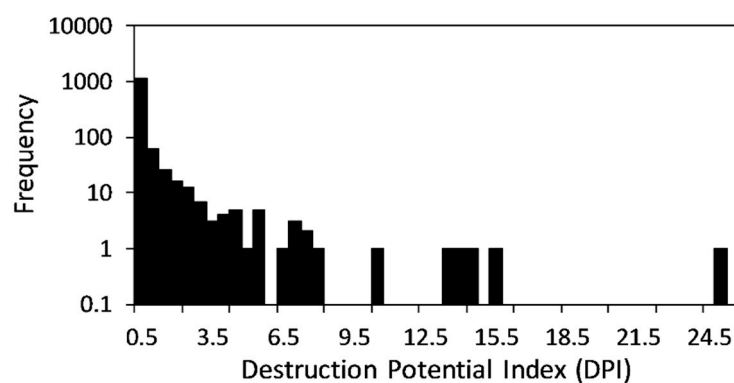


**Figure 4.** Frequency distribution of the DPI of 1285 TC tornadoes. The Y-axis is logarithmic.

**Table 13.** Top ten tornadoes (and ties) by DPI.

| TC Name | Month | Date | Year | F/EF | Length (km) | Width (m) | DPI | Bearing | Range | Casualties |
|---|---|---|---|---|---|---|---|---|---|---|
| Rita | 9 | 24 | 2005 | 2 | 29.0 | 731.2 | 24.55 | 73 | 348 | 3 |
| Andrea | 6 | 6 | 2013 | 1 | 30.4 | 643.5 | 15.11 | 59 | 233 | 0 |
| Lee | 9 | 5 | 2011 | 1 | 45.7 | 402.2 | 14.19 | 50 | 409 | 1 |
| Frances | 9 | 7 | 2004 | 3 | 11.3 | 804.3 | 14.00 | 61 | 480 | 1 |
| Cindy | 7 | 6 | 2005 | 2 | 14.5 | 804.3 | 13.50 | 70 | 256 | 0 |
| Rita | 9 | 25 | 2005 | 2 | 16.1 | 548.4 | 10.23 | 144 | 327 | 0 |
| Hermine | 9 | 8 | 2010 | 1 | 15.9 | 643.5 | 7.91 | 147 | 253 | 0 |
| Charley | 8 | 13 | 2004 | 2 | 67.6 | 91.4 | 7.16 | 60 | 198 | 0 |
| Ivan | 9 | 15 | 2004 | 2 | 11.3 | 548.4 | 7.16 | 65 | 323 | 9 |
| Ivan | 9 | 15 | 2004 | 2 | 12.9 | 457.0 | 6.82 | 61 | 318 | 3 |
| Rita | 9 | 25 | 2005 | 2 | 8.1 | 731.2 | 6.82 | 143 | 330 | 1 |

## 4. Discussion and Conclusions

　　The spatial distributions of tornado intensity and size in the US and in the TC environment were documented and analyzed in this study. The following are the key findings:

- Strong F/EF 2–3 TC tornadoes are more common (absolute and relative frequencies) at higher latitudes. The path length, path width, and DPI of the tornadoes also tend to increase in higher latitude regions.
- Strong F/EF 2–3 TC tornadoes are disproportionately common farther inland. The path length and width of the tornadoes also tend to be greater farther inland, along with their DPI.

- The path length and width of tornadoes are greatest, generally, in the EH of the TC environment, where TCs are most common. The relative frequency of strong F/EF 2–3 tornadoes is also greatest in these regions. The TC tornadoes that pose the greatest risk (i.e., those with the greatest DPI) tend to occur in a smaller region bound generally between 53° and 86° from N and between 285 km and 423 km from TC center.

Previous studies suggest that TCs produce more tornadoes when they track into higher latitudes and encounter westerly wind shear [6,28,29]. The increased proportion of strong F/EF 2–3 tornadoes, along with the greater median path lengths, path widths, and DPIs, in the 32° N–34° N and >34° N regions suggest that larger proportions of the tornadoes that TCs produce as they track into higher latitudes are stronger, larger, and potentially damaging (Figure 2; Table 1). This has been shown to be the case with Hurricane Ivan (2004) [8], but these results suggest that this may be a tendency for numerous TCs.

Previous studies show that TC tornadoes tend to occur near the coastline [3,5–7] and, furthermore, that this near-coastline clustering likely results from friction induced wind shear during landfall [10,11]. In addition to confirming this tendency (Figure 2; Table 3), this study also shows that the relative frequency of stronger and larger TC tornadoes increases with the distance from the coastline. Strong F/EF 2–3 tornadoes and those with larger median path lengths, widths, and DPIs were disproportionally common at inland locations (e.g., 200 km from the coastline).

Previous studies show that tornadoes are most common in the right half relative to TC motion or in the EH relative to N [3,6,7,10,11]. The results presented here support these observations (Figure 3; Tables 5, 7 and 11). They also show that tornadoes with the greatest potential to inflict damage (i.e., those with larger path coverage and stronger estimated intensities) also are most common in these regions of the TC environment. Furthermore, the most potentially damaging tornadoes with the greatest DPI are focused in a smaller region near the intersection of the NE and EoC quadrants, generally between 53° and 86° from N and between 285 km and 423 km from TC center. In addition to priming the NE and EoC quadrants for tornadogenesis [6,12,13], westerly wind shear may also contribute to the larger proportions of stronger and larger tornadoes near the intersection of these regions.

Some observations deviate from the aforementioned generalized patterns and would serve as insightful case studies. In particular, a relatively large proportion (10%) of the 100 tornadoes that occurred in the SoC quadrant were rated as strong F/EF 2–3. TC Rita (2005) produced four of the ten strong tornadoes in the SoC quadrant and, furthermore, produced a total of 39 tornadoes in the SoC quadrant. This means that approximately 40% of Rita's 98 tornadoes occurred in the SoC quadrant, which greatly exceeds the 8% in the SoC quadrant in the whole TCTOR database. It would also be insightful to evaluate changes in tornado risk (as a function of tornado frequency, tornado intensity, and tornado path characteristics) within the TC environment during different positions and stages of the TC lifecycle (e.g., near landfall and farther inland; tropical depressions and storms versus hurricane-strength). Further stratification of the TCTOR database, however, is problematic because of reduced sample sizes. Nonetheless, additional documentation and analysis of the distributions of TC tornadoes and their intensity and size characteristics will benefit efforts to develop TC tornado risk and vulnerability models, similar to those developed for non-TC tornadoes [18,30–34]. A better understanding of the factors that contribute to the number of tornadoes produced by TCs will also benefit these modeling efforts. For example, some TCs, such as Ivan (2004), Frances (2004), and Rita (2005), produce many tornadoes whereas others, such as Dolly (1996), Charley (1997), and Dennis (1999), produce a few or none. Inclusion of factors that distinguish between TCs that produce many and TCs that produce few would refine tornado risk models.

**Author Contributions:** T.W.M. conceived and designed the study; T.W.M., R.A.B., and N.J.S. managed the data and performed the analyses; and T.W.M. and N.J.S. wrote the manuscript.

**Conflicts of Interest:** The authors declare no conflict of interest.
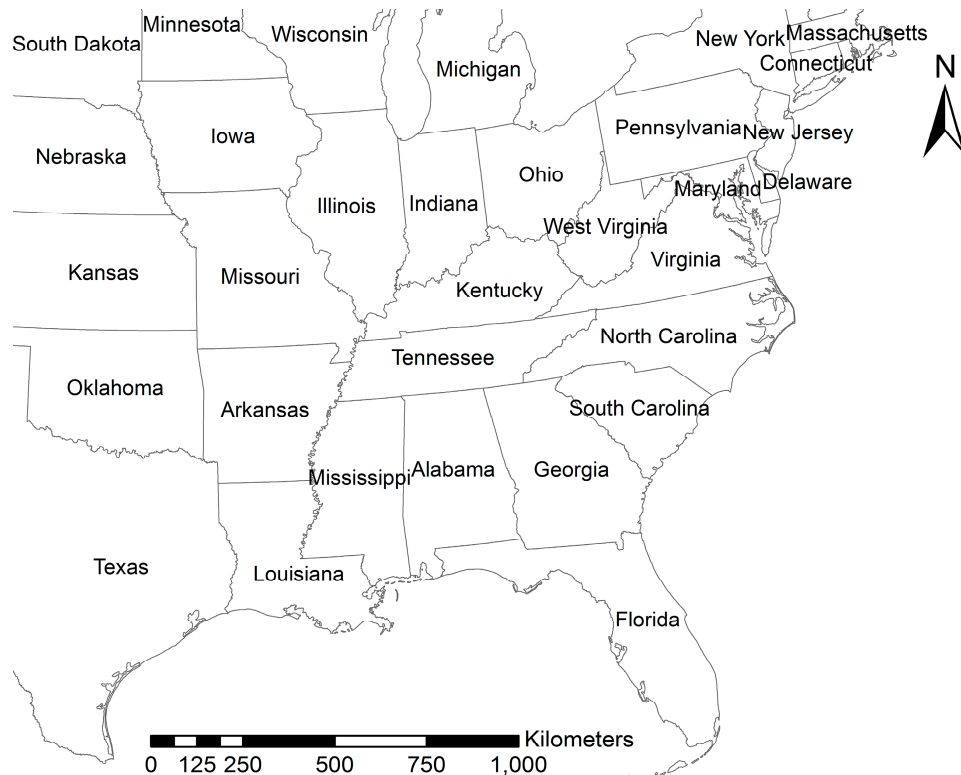
## Appendix A



**Figure A1.** Names of states relevant to this study.

## References

1. Moore, T.W.; Dixon, R.W. Tropical cyclone-tornado casualties. *Nat. Hazards* **2012**, *61*, 621–634. [CrossRef]
2. Stewart, S.R. Tropical Cyclone Report-Hurricane Cindy. National Hurricane Center, 2006. Available online: http://www.nhc.noaa.gov/pdf/TCR-AL032005_Cindy.pdf (accessed on 22 August 2017).
3. Weiss, S.J. On the operational forecasting of tornadoes associated with tropical cyclones. In Proceedings of the 14th Conference on Severe Local Storms, Indianapolis, IN, USA, 29 October–1 November 1985; pp. 293–296.
4. Schultz, L.A.; Cecil, D.J. Tropical cyclone tornadoes, 1950–2007. *Mon. Weather Rev.* **2009**, *137*, 3471–3484. [CrossRef]
5. Moore, T.W.; Dixon, R.W. Climatology of tornadoes associated with Gulf Coast-landfalling hurricanes. *Geogr. Rev.* **2011**, *101*, 371–395. [CrossRef]
6. McCaul, E.W., Jr. Buoyancy and shear characteristics of hurricane-tornado environments. *Mon. Weather Rev.* **1991**, *119*, 1954–1978. [CrossRef]
7. Edwards, R. Tropical cyclone tornadoes: A review of knowledge in research and prediction. *Electron. J. Severe Storms Meteorol.* **2012**, *7*, 1–33.
8. Moore, T.W.; Dixon, R.W. A spatiotemporal analysis and description of Hurricane Ivan's (2004) tornado clusters. *Pap. Appl. Geogr.* **2015**, *1*, 192–196. [CrossRef]
9. Moore, T.W.; Dixon, R.W.; Sokol, N.J. Tropical cyclone Ivan's tornado cluster in the Mid-Atlantic Region of the United States on 17–18 September 2004. *Phys. Geogr.* **2016**, *37*, 210–227. [CrossRef]
10. Novlan, D.J.; Gray, W.M. Hurricane-spawned tornadoes. *Mon. Weather Rev.* **1974**, *102*, 476–488. [CrossRef]
11. Gentry, R.C. Genesis of tornadoes associated with hurricanes. *Mon. Weather Rev.* **1983**, *111*, 1793–1805. [CrossRef]
12. Molinari, J.; Vollaro, D. Distribution of helicity, CAPE, and shear in tropical cyclones. *J. Atmos. Sci.* **2010**, *67*, 274–584. [CrossRef]

13. Molinari, J.; Romp, D.M.; Vollaro, D.; Nguyen, L. CAPE in tropical cyclones. *J. Atmos. Sci.* **2012**, *69*, 2452–2463. [CrossRef]

14. Sueki, K.; Niino, H. Toward better assessment of tornado potential in typhoons: Significance of considering entrainment effects for CAPE. *Geophys. Res. Lett.* **2016**, *43*, 12597–12604. [CrossRef]

15. Colquhoun, J.R.; Riley, P.A. Relationships between tornado intensity and various wind and thermodynamic variables. *Weather Forecast.* **1996**, *11*, 360–371. [CrossRef]

16. Thompson, R.L.; Edwards, R.; Hart, J.A.; Elmore, K.L.; Markowski, P. Close proximity soundings within supercell environments obtained from the Rapid Update Cycle. *Weather Forecast.* **2003**, *18*, 1243–1261. [CrossRef]

17. Doswell, C.A., III; Edwards, R.; Thompson, R.L.; Hart, J.A.; Crosbie, K.C. A simple and flexible method for ranking severe weather events. *Weather Forecast.* **2006**, *21*, 939–951. [CrossRef]

18. Coleman, T.A.; Dixon, P.G. An objective analysis of tornado risk in the United States. *Weather Forecast.* **2014**, *29*, 366–376. [CrossRef]

19. Edwards, R. Tropical Cyclone Tornado Records for the Modernized NWS Era. Available online: http://ams.confex.com/ams/25SLS/techprogram/paper_175269.htm (accessed on 20 June 2017).

20. Edwards, R. TCTOR Database. Available online: http://www.spc.noaa.gov/misc/edwards/TCTOR/tctor.xls (accessed on 26 August 2017).

21. Edwards, R. README.TXT for SPC TCTOR Database. Available online: www.spc.noaa.gov/misc/edwards/TCTOR/readme.txt (accessed on 26 August 2017).

22. McCarthy, D.W. NWS Tornado Surveys and the Impact on the National Tornado Database. 1st Symposium F-Scale and Severe-Weather Damage Assessment, Long Beach, CA, USA, 2003; American Meteorological Society. Available online: http://www.spc.noaa.gov/publications/mccarthy/f-scale.pdf (accessed on 22 August 2017).

23. Doswell, C.A., III; Brooks, H.A.; Doztek, N. On the implementation of the enhanced Fujita scale in the USA. *Atmos. Res.* **2009**, *93*, 564–674. [CrossRef]

24. Edwards, R.; LaDue, J.G.; Ferree, J.T.; Scharfenberg, K.; Maier, C.; Coulbourne, W.L. Tornado intensity estimation: Past, present, and future. *Bull. Am. Meteorol. Soc.* **2013**, *94*, 641–653. [CrossRef]

25. Thompson, R.L.; Vescio, M.D. The destruction potential index—A method for comparing tornado days. In Proceedings of the 19th Conference on Severe Local Storms, Minneapolis, MN, USA, 14–18 September 1998; American Meteorological Society: Boston, MA, USA, 1998.

26. Fricker, T.; Elsner, J.B.; Jagger, T.H. Population and energy elasticity of tornado casualties. *Geophys. Res. Lett.* **2017**, *44*, 3941–3949. [CrossRef]

27. Ashley, W.S.; Strader, S.M. Recipe for disaster: How the dynamic ingredients of risk and exposure are changing the tornado disaster landscape. *Bull. Am. Meteorol. Soc.* **2016**, *97*, 767–786. [CrossRef]

28. Verbout, S.M.; Schulz, D.M.; Leslie, L.M.; Brooks, H.E.; Karoly, D.J.; Elmore, K.L. Tornado outbreaks associated with landfalling hurricanes in the North Atlantic basin: 1954–2004. *Meteorol. Atmos. Phys.* **2007**, *97*, 255–271. [CrossRef]

29. Moore, T.W.; Dixon, R.W. Pattern in 500 hPa geopotential height associated with temporal clusters of tropical cyclone tornadoes. *Meteor. Appl.* **2015**, *22*, 314–322. [CrossRef]

30. Romanic, D.; Maryam, R.; Wu, C.-H.; Michel, G. Oklahoma tornado risk and variability: A statistical model. *Int. J. Disaster Risk Reduct.* **2016**, *16*, 19–32. [CrossRef]

31. Standohar-Alfano, C.D.; van de Lindt, J.W. Empirically based probabilistic tornado hazard analysis of the United States using 1973–2011 data. *Nat. Hazards Rev.* **2015**, *16*. [CrossRef]

32. Strader, S.M.; Pingel, T.J.; Ashley, W.S. A monte carlo model for estimating tornado impacts. *Meteorol. Appl.* **2016**, *23*, 269–281. [CrossRef]

33. Dixon, R.W.; Moore, T.W. Tornado vulnerability in Texas. *Weather Clim. Soc.* **2012**, *4*, 59–68. [CrossRef]

34. Elsner, J.B.; Jagger, T.H.; Fricker, T. Statistical models for tornado climatology: Long and short-term views. *PLoS ONE* **2016**, *11*, e0166895. [CrossRef]